

Azimuth Variation in Microwave Backscatter over the Greenland Ice Sheet

Ivan S. Ashcraft and David G. Long

Brigham Young University Microwave Earth Remote Sensing Laboratory
459 Clyde Building, Provo, UT 84602
801-378-4884, FAX: 801-378-6586, e-mail: ashcraft@ee.byu.edu

Abstract – Scatterometer backscatter measurements are becoming an important tool for monitoring the dynamic behavior of the Greenland ice sheet. However, most Greenland studies assume constant backscatter for varying azimuth angles. Detailed analysis of scatterometer data sets show non-negligible (1-2 dB) azimuth modulation. The magnitude and orientation of the azimuth modulation observed by SeaWinds, NSCAT, and ERS are documented herein. The dominate factor is second order azimuth modulation, which is largest for C-band (ERS). For SeaWinds, the h-pol azimuth modulation is larger than for v-pol.

I. INTRODUCTION

THE accumulation/ablation balance of the Greenland Ice Sheet is considered a sensitive indicator of global climate change. Although primarily designed for measuring vector wind speeds over the ocean, wind scatterometers have proven to be valuable tools for many Greenland and other cryosphere studies. SAR and radiometers are effectively being used in similar studies. These scatterometers are effective tools in these studies because they provide frequent large scale coverage of the entire ice sheet. Currently, however, most studies of Greenland using microwave measurements assume no variation in backscatter with azimuth angle. Recently, significant azimuth variation has been documented over Antarctica [1], [2]. An investigation of azimuth variation over Greenland provides for both an increased understanding of the ice sheet properties and the ability to account for azimuth variation in accumulation, ablation, and other studies.

In this paper, azimuth modulation over Greenland is documented for SeaWinds on QuikSCAT, the NASA scatterometer (NSCAT), and ERS-2 scatterometer. First, raw data samples are shown, then a simple model is introduced, and finally the azimuth modulation is mapped for each sensor over the entire ice sheet.

II. RAW DATA

Figure 1 shows σ° measurements over a Greenland study region for SeaWinds, NSCAT, and ERS as a function of azimuth angle. The dark line in each plot indicates the least squares model fit which will be discussed in the next section. The raw measurements are taken from a 9×9 km area in the north-east portion of the Greenland ice sheet (see Fig. 2). For each sensor, different day ranges were used. SeaWinds uses 2 days of data (J.D. 349-350, 1999), NSCAT uses 30 days of data (J.D. 331-360, 1996), while ERS uses 11 days (J.D. 348-358, 1999). Because NSCAT and ERS make measurements at a wide range of incidence angles, these measurements were normalized to

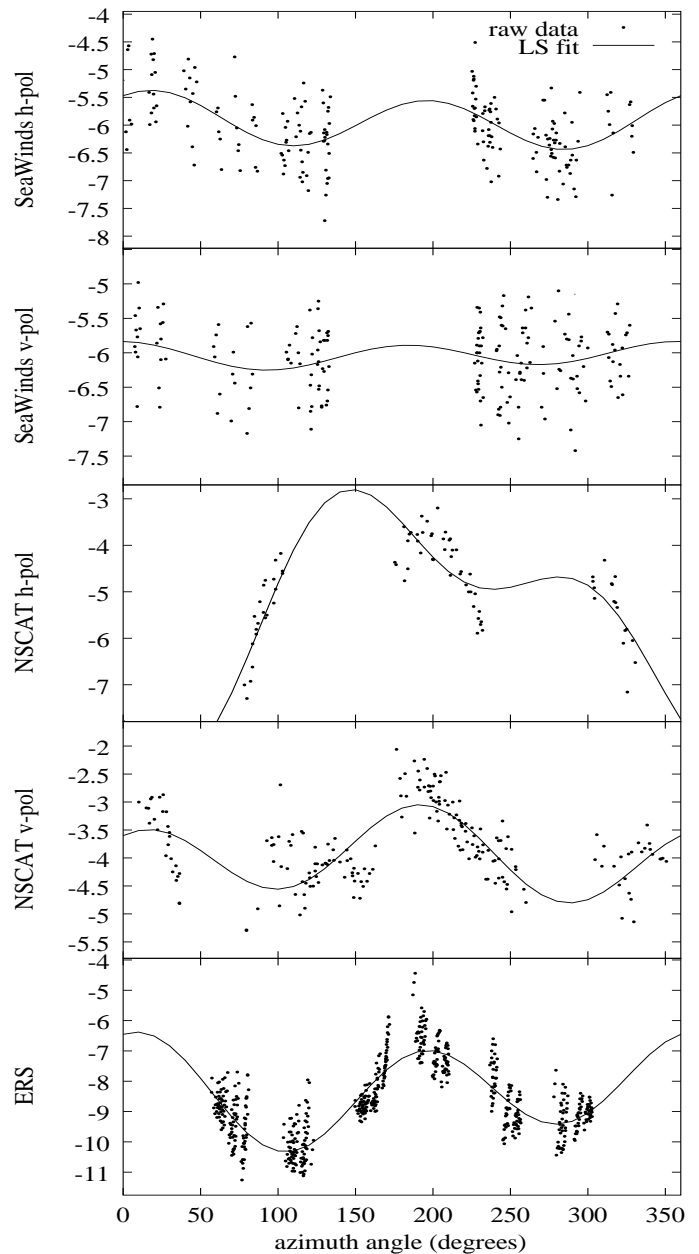


Fig. 1. Five sets of σ° measurements over the Greenland ice sheet. The dark line represents a least squares fit to the data using a simple model (see text). The vertical axis represents σ° measured in dB. The study region is a 9×9 km area in North-East Greenland in the dry snow zone (See Fig. 2). For NSCAT and ERS the measurements are normalized to 40° incidence angle.

40° incidence angle before plotting. The incidence angle dependence used for the normalization was calculated using the SIR algorithm [3]. The raw measurements shown in Fig. 1 show some of the largest azimuth modulation observed over the Greenland ice sheet. It is interesting to note that the orientation of the azimuth modulation is similar for all of the sensors, but the magnitude varies depending on sensor and polarization.

For SeaWinds the azimuth modulation is relatively small. There is a ~ 1.0 dB peak-to-peak variation for h-pol; for v-pol the variation is about half this. SeaWinds measurements are at fixed incidence angles with h-pol $\theta \approx 46.3^\circ$ and v-pol $\theta \approx 54.1^\circ$. One of the benefits of SeaWinds data is the wide range of azimuth angles observed. With only two days of data, the coverage is sufficient to perform a well-conditioned least squares fit of the azimuth model. In the raw data shown for SeaWinds, a gap in the measurements is observed around 180° . This is because the north end of Greenland is at such a high latitude. For regions further South the entire azimuth range is covered.

The NSCAT measurements also display significant azimuth modulation; however, for h-pol measurements the limited azimuth sampling limits potential conclusions. NSCAT has eight antenna beams, two h-pol and six v-pol. With only two h-pol beams, four azimuth angles are observed (two for ascending passes, and two for descending). The h-pol model fit is poor, but by close inspection, one can see that a model fit with orientation similar to the other sensors would also fit the NSCAT h-pol measurements. The NSCAT v-pol data better covers the whole azimuth range [2].

ERS makes measurements at six azimuth angles which is sufficient for a well-conditioned model fit. The azimuth modulation observed for ERS (~ 4 dB peak-to-peak) is much larger than for the Ku-band instruments. ERS measures σ° for v-pol only.

III. MODEL

A simple second order Fourier series is used to model of the σ° azimuth modulation over Greenland. This model is the same as the “F-model” used by Long and Drinkwater in their study of azimuth modulation over Antarctica [2]. This model is able to identify both the magnitude and orientation of the first and second order azimuth modulations. The model can be written

$$\sigma^\circ = A_0 + A_1 \cos(\phi + \phi_1) + A_2 \cos(2\phi + \phi_2) + B(\theta - \theta_{\text{ref}})$$

where the coefficients are defined as follows:

- A_0 - incidence angle normalized average value of σ° ,
- A_1 - first order azimuth modulation magnitude,
- ϕ_1 - first order azimuth modulation orientation,
- A_2 - second order azimuth modulation magnitude,
- ϕ_2 - second order azimuth modulation orientation,
- B - incidence angle dependence of σ° ,
- θ - incidence angle, and
- θ_{ref} - reference angle.

The model neglects any incidence angle dependence of A_1 and A_2 . This is necessary because there is insufficient data to perform a fit to a model including these dependencies. For NSCAT and ERS $\theta_{\text{ref}} = 40^\circ$. Because SeaWinds only makes measurements at a single incidence angle for each polarization, B is not calculated. Therefore the final term is dropped, effectively equivalent to setting θ_{ref} to the SeaWinds incidence angle.

IV. IMAGES

A least-squares fit to the azimuth modulation model is used to create images of each model parameter. The images for each of the sensors are shown in Fig. 2. The NSCAT h-pol images were not included because of the ill-conditioned least-squares fit mentioned previously.

The A_0 images are similar for all of the sensors with the only significant difference being a offset in the mean σ° value. This offset is caused by differences in the values of θ_{ref} for SeaWinds h-pol, SeaWinds v-pol, and NSCAT, and a difference in frequency for ERS. We note the variation in A_0 in the different snow zones. The bright area around the periphery of the ice sheet is the wet snow and percolation zone, and the inner darker region is the dry snow zone [4].

The A_1 and A_2 images show the magnitude of the first and second order azimuth modulation respectively. For the Ku-band sensors, there is moderate first order azimuth modulation on the western border between the dry snow zone and percolation zone. ERS shows first order modulation in the same area, only extending further into the dry snow zone. First order modulation is observed by ERS over a much larger area than is visible for NSCAT and SeaWinds.

The second order azimuth modulation (term A_2) is much larger than the first order (term A_1) for all of the sensors except SeaWinds v-pol. The key difference between SeaWinds v-pol and NSCAT v-pol measurements is the incidence angle. The ERS second order azimuth modulation is 1 dB or greater over a large portion of the dry snow zone.

The ϕ_1 and ϕ_2 images show the orientation of the azimuth modulation. These images show that the orientation of the azimuth modulation is highly correlated, which implies that the observed azimuth modulation is real, not just the effects of noise. It is worthy to note that even in regions where the azimuth modulation is small, the orientation of the modulation is still highly correlated.

V. SUMMARY

Scatterometer measurements display azimuth modulation throughout the Greenland ice sheet. Using a simple azimuth model, images of each model parameter were created. These images show azimuth modulation largest in the lower regions of the dry snow zone. The second order modulation dominates. For ERS, the second order azimuth modulation has a magnitude larger than 1 dB throughout significant portions of the dry snow zone. The orientation of the azimuth modula-

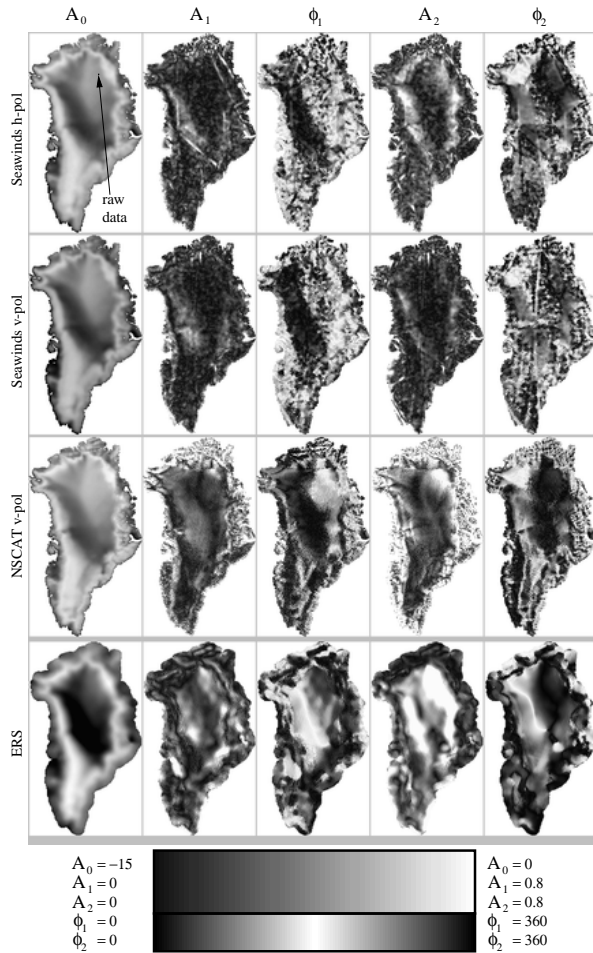


Fig. 2. Images showing azimuth modulation observed by SeaWinds, NSCAT, and ERS. Each row is for a different sensor. Each column is for a different model coefficient.

tion is highly correlated, even in regions where the modulation magnitude is small. The similar results from the three instruments suggests that the azimuth modulation is caused by some physical property of the ice sheet surface such as sastrugi or some other snow/ice formation [2].

REFERENCES

- [1] N. Young, D. Hall, and G. Hyland, "Directional anisotropy of C-band backscatter and orientation of surface microrelief in east antarctica," in *Proceedings of the First Australian ERS Symposium*, pp. 117–126, Feb. 1996.
- [2] D. G. Long and M. R. Drinkwater, "Azimuth variation in microwave scatterometer and radiometer data over Antarctica," *IEEE Trans. on Geosci. and Rem. Sens.*, vol. 38, pp. 1857–1870, July 2000.
- [3] D. G. Long, P. J. Hardin, and P. T. Whiting, "Resolution enhancement of spaceborne scatterometer data," *IEEE Trans. on Geosci. and Rem. Sens.*, vol. 31, no. 3, pp. 700–715, 1993.
- [4] D. G. Long and M. R. Drinkwater, "Greenland ice-sheet surface properties observed by the Seasat-A scatterometer at enhanced resolution," *J. of Glaciology*, vol. 40, no. 135, pp. 213–230, 1994.